Desalination and Water Treatment
www.deswater.com
doi: 10.1080/19443994.2015.1005155

57 (2016) 5623–5635
March

Taylor & Francis
Taylor & Francis Group

Removal of nickel (II) ion by adsorption on coconut copra meal biosorbent

Misbah Saleem, Natee Wongsrisujarit, Siwarutt Boonyarattanakalin*

School of Bio-Chemical Engineering and Technology, Sirindhorn International Institute of Technology, Thammasat University, Khlong Nueng, Khlong Luang 10120, Pathum Thani, Thailand, Tel. +66 2 986 9009, ext. 2305; email: siwarutt@siit.tu.ac.th (S. Boonyarattanakalin)

Received 7 October 2014; Accepted 28 December 2014

ABSTRACT

The present study explores the utilization of biomass from coconut copra meal (CCM) as a biosorbent to remove nickel (II) ions (Ni(II)) from aqueous solutions. CCM biomass can be processed into a sorbent easily due to its soft nature derived from the molecular composition of β-mannan which is different from β-glucose found in other cellulosic biomass. The sub-micrometer structures on the prepared CCM sorbent were revealed by SEM. The prepared CCM sorbent was porous with many openings. Investigations on the effects of solution pH, biosorbent dose, initial metal concentration, contact time, and temperature were carried out to determine the optimum biosorption conditions in a batch system. The kinetics, adsorption isotherms, and adsorption thermodynamics of Ni(II) biosorption onto the CCM biosorbent were investigated. The experimental data were analyzed for the biosorption kinetics by using the pseudo-first-order, pseudo-second-order, and intraparticle diffusion models. It was observed that the pseudo-second-order model fitted better with the kinetics data of Ni(II) biosorption as compared to other models. Adsorption isotherm studies revealed that the Langmuir isotherm model showed a better fit for the experimental data when compared to the Freundlich isotherm model. The maximum monolayer capacity of CCM for Ni(II) was determined to be 3.77 mg/g. From the thermodynamic studies, the positive value of ΔH° indicates that the adsorption is an endothermic process and mainly attributed by a physical sorption. The negative values of ΔG° indicate that the process is spontaneous. The desorption process was evaluated and it was found that 0.1 M HNO_3 was able to desorb almost 100% of Ni(II) that adsorbed on the CCM biomass. The study of co-ions effect showed small decreases in biosorption of Ni(II) in the presence of Co(II), and more decreases with the Pb(II) presence. This study reveals the feasibility of an economical process to remove Ni(II) from wastewater by the CCM biosorbent.

Keywords: Biosorption; Coconut copra meal (CCM); Nickel ions; Biomass; Nickel removal

1. Introduction

Rapid industrialization has accented a significant threat to human health and several ecosystems with the accumulation of heavy metals. Heavy metals are toxic as they persist in nature for a long time due to their non-biodegradable nature. The ions of these metals possess great chronic toxicity to humans and animals. Heavy metals of great concerns are lead, copper, nickel, zinc, mercury, cadmium, and arsenic. Some heavy metal ions, such as mercury ions in an

*Corresponding author.

aqueous system, can undergo a change in oxidation state from less toxic to more toxic states.

Nickel ion contaminations in water are commonly found in wastewater from nickel plating, welding, oil refinery, paint production, and mining. The increased levels of exposure to Ni(II) cause nausea, vomiting, diarrhea, skin dermatitis, renal edema, and pulmonary fibrosis [1–4]. The chronic toxicity of Ni(II) ion includes lung fibrosis and cancer of the respiratory tract [5]. According to the World Health Organization, the permissible limit of nickel in drinking water is 0.07 mg/L [6]. Therefore, it is important to efficiently remove the nickel ions from wastewater coming out of industries. For this purpose, many strategies to remove nickel ions from industrial wastewater have been developed including reverse osmosis, electrodialysis, ion exchange, chemical precipitation, and phytoremediation [7]. Unfortunately, high cost, low efficiency at low heavy metal concentrations (1–100 mg/L), sludge formation, and additional chemical requirements make these processes less feasible [7–10].

Biosorption is an alternative process that can overcome these shortcomings of traditional methods with low cost and high efficiency. Biosorption may occur through one or a combination of several processes, which are diffusion, ion exchange, physical or chemical adsorption, precipitation, chelation and/or complexation [11,12]. Biosorbents used for biosorption are mostly composed of polysaccharides, lipids, and proteins that contain different functional groups such as carbonyl, phenolic, carboxylate, hydroxyl, amido, amino, sulfate and phosphate groups that play a role in bioaccumulation of heavy metals from wastewaters [13,14].

Coconut copra meal (CCM) is a waste of the coconut oil extracting industry. CCM is readily and abundantly available in tropical countries including Indonesia, Philippines, India, Brazil, Sri Lanka, and Thailand. During the production of coconut oil, a large amount of CCM is generated as waste. A very small proportion of this waste is used as fodder for pigs and horses. The major component of the native CCM is polysaccharides, and other minor compositions are lipids, proteins, and dietary fibers [15]. Various functional groups on the surface of CCM could participate in binding with heavy metal ions.

The major carbohydrate component of CCM is mannan, and other minor carbohydrate components are comprised of cellulose, arabinoxylogalactan, galactomannan, arabinomannogalactan, and galactoglucomannanose [16]. Although the active functional groups such as the hydroxyl and carboxylic acid moieties are present in CCM, the spatial arrangements of these functional groups on the mannose units are different from typical cellulosic biomass which is mainly composed of glucose units. Previously, only cadmium (II) ion was found to be adsorbed on CCM [15,17]. The present study was carried out to evaluate the potential of CCM to remove Ni(II) from aqueous solutions. Effects of various parameters on Ni(II) biosorption such as biomass dose, initial pH, initial metal ion concentration, contact time, and temperature were studied. To understand the biosorption process, adsorption isotherms, kinetics, and thermodynamic studies were carried out.

2. Materials and methods

2.1. Biomass preparation

CCM was obtained after cold pressing of coconut meal from Tropicana Oil Co. Ltd, Thailand. The copra meal was blended in a food-processing blender and boiled six times to remove trace amounts of oil. The copra meal was dried at 70˚C in a hot air oven. The copra meal was then soaked with 0.02 M HCl overnight to dissolve plant debris, lignin, and other plant materials. After that, the copra meal was filtered off, and it was washed with reverse osmosis water several times until the pH of the washing water became neutral. The washed copra meal was dried at 70˚C in a hot air oven for 24 h and then sieved to obtain the biomass adsorbent with 60 mesh (≤250 μm) particle size. The CCM biomass was stored in air tight containers for later usages.

2.2. Biomass characterizations

2.2.1. Scanning electron microscope

The prepared CCM sorbent was characterized by electron microscope (SEM JSM-5410, JEOL Ltd, Tokyo, Japan) equipped with an energy dispersive X-ray spectrometer (EDS link ISIS300).

2.2.2. Fourier transform infrared spectroscopy

The infrared spectra of the biomass adsorbent were characterized by NICOLET™ 6700 Spectrometer. The pressed pellet sample was prepared by grinding and pressing the biomass with KBr.

2.3. Chemicals

All chemicals used were of analytical reagent grade. Stock solution (1 g/L) of Ni(II) was prepared by dissolving the appropriate amount of nickel nitrate hexahydrate ($Ni(NO_3)_2{\cdot}6H_2O$) in 1.0 L of deionized

water. The stock solution was stored at 4°C and further required dilutions were carried out accordingly, from the stock solution. HCl and NaOH aqueous solutions (0.1 M) were used for pH adjustment.

2.4. Adsorption experiments

Batch biosorption experiments were carried out to evaluate the potential of CCM to remove Ni(II) from aqueous solutions and to determine the effects of initial solution pH, initial Ni(II) concentration, CCM biosorbent dose, temperature, and contact time on the biosorption capacity of the CCM. All batch experiments were carried out at the 50 mL of nickel solution scale. The Ni(II) solution was incubated in an Erlenmeyer flask with a certain amount of biosorbent at 26°C. The initial pH of the Ni(II) solution was adjusted to a certain value by using 0.1 M NaOH or HCl aqueous solutions. The mixture was then agitated for a specified time period at 150 rpm. After agitation, the final pH of the solution was recorded. The mixture was filtered and supernatant was analyzed for the Ni(II) by an atomic absorption spectrometer (AAS, PerkinElmer AAnalyst-200). All experiments were conducted in triplicate including the controls. The amount of Ni(II) adsorbed by CCM was calculated using Eqs. (1) and (2):

$$q_e = \frac{C_1 - C_2}{M} \times V \quad (1)$$

where, q_e is the metal uptake capacity (mg/g) of CCM for Ni(II), V is the solution volume (L), C_1 and C_2 are the initial and final concentrations (mg/L) of Ni(II), and M is the mass (g) of CCM used for Ni(II) biosorption.

$$\text{Adsorption efficiency } (\%) = \frac{C_1 - C_2}{C_1} \times 100 \quad (2)$$

2.4.1. Effect of initial pH on Ni(II) adsorption

50 mL of 120 mg/L Ni(II) solution was aliquoted into a 250 mL Erlenmeyer flask containing 1 g of the CCM biosorbent. The pH of Ni(II) solutions was adjusted by 1 M NaOH and/or 1 M HCl. The flasks of mixtures were placed on a rotary shaker at 150 rpm for 2 h. All experiments were conducted at 26°C.

2.4.2. Effect of adsorbent dose

50 mL of 120 mg/L Ni(II) was aliquoted into a 250 mL Erlenmeyer flask containing different amounts of biosorbent. The pH of the solutions was adjusted to 5. The samples were shaken at 150 rpm, 26°C for 2 h.

2.4.3. Effect of contact time and kinetics studies

In the kinetic experiments, 1.0 g of biomass was added to a 250 mL Erlenmeyer flask containing the metal solutions at 60, 100, and 120 mg/L (50 mL). The initial pH was maintained at the optimum value of 5.0. All flasks were shaken at 150 rpm at 26°C. Samples were taken at the indicated periodic time intervals.

2.4.4. Equilibrium studies

In the adsorption isotherm experiments, 1 g of biomass was added to a 250 mL Erlenmeyer flask containing 50 mL of a Ni(II) solution with various concentrations. The pH was adjusted to 5. All samples were shaken at 150 rpm, 26°C for 2 h.

2.4.5. Effect of temperature

For the study of temperature effect on the adsorption, 1 g of biomass was added to a 250 mL Erlenmeyer flask containing 50 mL of Ni(II) solution of varying concentrations (40, 60, 100, and 120 mg/L). The pH was adjusted to 5. All samples were shaken at 150 rpm and at a specific temperature (15, 35, and 45°C) for 6 h. After incubation, the biomass was filtered out and the filtrate was analyzed for Ni(II) concentration.

2.4.6. Desorption studies

The biomass that was used to adsorb Ni(II) from the solution was used to conduct the desorption experiment. For the adsorption process, 1 g of biomass was added to 50 mL of 120 mg/L Ni(II) solution at 25°C and the solution pH was adjusted to 5. The mixture was shaken at 150 rpm for 6 h. After that, the biomass was filtered and used for desorption. In the desorption experiment, 50 mL of 0.1 M HNO_3 was added to the filtered biomass. The mixture was then shaken at 150 rpm for 6 h at 25°C. After incubation, the biomass was filtered out and weighted, and the filtrate was analyzed for Ni(II) concentration.

2.4.7. Quantification of Ni(II)

Atomic absorption spectroscopy (AAS, PerkinElmer AAnalyst-200) was used to determine the remaining concentration of Ni(II) in the filtrates. The calibration curve was constructed based on the standard nickel solutions. The calibration curve must have the correlation coefficient value of 0.998–1.0.

3. Results and discussion

3.1. Biomass preparation and characterizations

It is important to point out the uniqueness of the molecular structure of CCM which makes it different from other cellulosic biomass. The major monosaccharide component of CCM is mannose with much less lignin, resulting in a much softer biomass than other cellulosic counterparts. The softness of CCM allows easier conversion of the raw biomass into a sorbent since this process requires less powerful grinding.

CCM biomass was characterized by scanning electron microscopy (SEM) and energy dispersive X-ray spectroscopy (EDX). SEM analysis confirmed that the sizes of CCM biomass particles were less than 250 μm (Fig. 1(a)). The micrographs of the CCM show porous surface morphology of openings in alternate with submicrometer size of protruding microstructures that provide larger surface area available for adsorption (Fig. 1). The EDX analysis revealed the presence of minor elements including calcium and copper, in addition to the major elements which are carbon and oxygen. The presence of alkaline earth on the surface of CCM suggests the possibility of a cationic exchange during biosorption of Ni(II) onto CCM biomass [18]. The carbon to oxygen weight ratio of approximately 1.7:1 was observed on the surface of the CCM biosorbent.

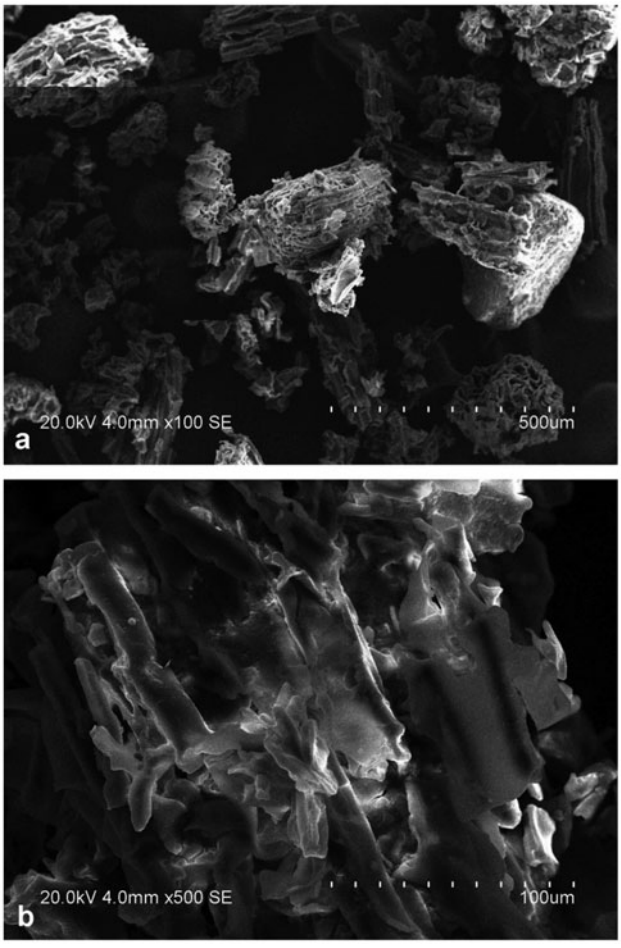

Fig. 1. Scanning electron micrographs of CCM biomass at (a) 100× and (b) 500× magnifications.

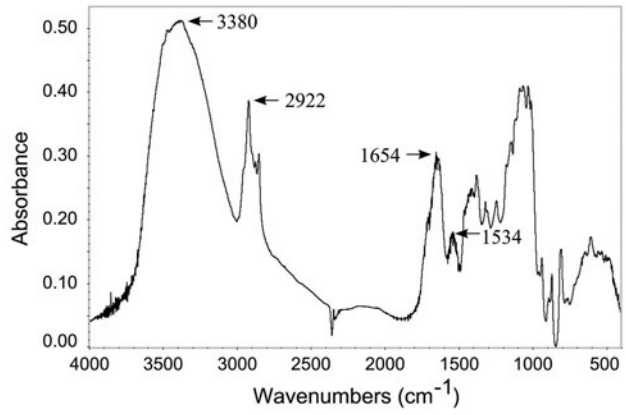

Fig. 2. FTIR spectrum of the coconut copra meal biosorbent.

Table 1
Functional of groups on coconut copra meal biomass adsorbent identified by FTIR

Wave number (cm^{-1})	Assignment
3,380.2	Bonded hydroxyl group, –NH stretching
2,922.3	C–H stretching
1,654.1	C=O chelate stretching, Amide I band
1,534.4	Amide II band

The Fourier transform infrared spectroscopy (FTIR) was used to determine the functional groups found on the biomass surface. Fig. 2 shows the FTIR peaks of the CCM biomass. The functional groups found on the surface of biomass were the hydroxyl group (3,380 cm^{-1}), –NH (3,380 cm^{-1}), C–H (2,922 cm^{-1}), amide (1,534 cm^{-1}), and C=O (1,654 cm^{-1}) [19]. The wave numbers are assigned for each function group as shown in Table 1.

3.2. Effect of pH

Initial pH of the solution is very significant as it has a direct influence on sorption of heavy metal ions by a sorbent. The effect of initial pH on the

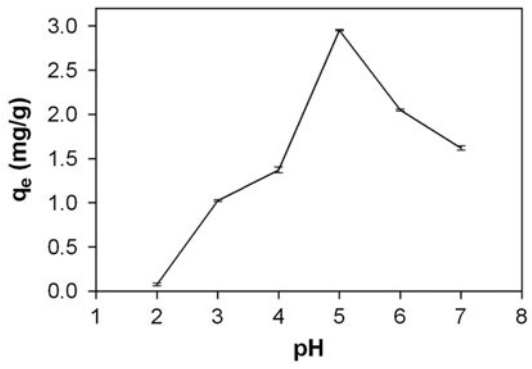

Fig. 3. The effect of pH on the biosorption of Ni(II) by CCM as biosorbent (biomass dose = 1.0 g/50 mL; Ni(II) concentration = 120 mg/L; contact time = 2 h).

biosorption of Ni(II) was investigated with a nickel nitrate solution by varying its pH from 2 ± 0.02 to 7 ± 0.02 (Fig. 3). The pH profile for the Ni(II) biosorption using the CCM as a biosorbent showed that as the pH of the solution increased from 2 to 5, the biosorption of Ni(II) significantly increased. The maximum Ni(II) biosorption was found to be at pH 5.0 (q_e = 2.95 mg/g). At low pH, most of the binding sites were occupied by H^+ ions, therefore, less biosorption took place. As the pH increased, the surface of biomass became more negatively charged; so, greater biosorption for Ni(II) at the higher pH value (pH 5.0) was observed [20]. However, further increases in pH value (>5.0) showed a decrease in Ni(II) biosorption possibly due to the formation of soluble hydroxide complexes of Ni (II), which competes with the biosorption of Ni(II) by biomass [21]. Therefore, the optimum pH value used for next biosorption experiments was at 5. Similar results of the effect of pH on the biosorption of Ni(II) were observed for Ni(II) biosorption using dried green alga [22], activated sludge [23], and waste tea material [24].

The final pH, or equilibrium pH, after the adsorption of Ni(II) onto CCM biomass, was also investigated. The initial pH of the mixtures of CCM biomass in different concentrations of Ni(II) solutions were adjusted to 5. After the incubation, the equilibrium pH for all samples was found to be from 4.8 to 5, which was slightly lower than the initial pH of 5. The decrease in pH may reflect the mechanism of Ni(II) adsorption onto the biomass. As suggested by Kadirvelu et al. the adsorption of Ni(II) onto the biomass is possibly due to the ion-exchange process [25]. The H^+ ions from the functional groups on the biomass were released while the Ni(II) was adsorbed onto the biomass. As a result, the final pH solution was slightly lower than the initial pH.

3.3. Effect of biomass dose

The effect of biomass dosage on the Ni(II) biosorption using CCM as biomass was studied using different biomass doses (0.1–2.0 g/50 mL) and the results are presented in Fig. 4. The results showed that the biomass dose directly influenced the adsorption efficiency of Ni(II). The Ni(II) adsorption efficiency increased from 11.22 to 47.20% with an increase in biomass dose from 0.1 to 1.0 g of CCM, while the maximum uptake capacity of Ni(II) by CCM is 6.73 mg/g at 0.1 g of biomass dose. After a further increase in biomass dose to more than 1.0 g, the adsorption efficiency did not increase, and a slight decrease in the Ni(II) biosorption to 46.15% at a biomass dose of 2.0 g/50 mL was observed. The initial increase in adsorption efficiency is attributed to the fact that the increase in biomass dose results in an increase in the number of available binding sites for Ni(II). However, at the biomass doses of more than 1.0 g, a further increase in biomass dose showed a slight decrease in adsorption efficiency. This was probably due to the aggregation of biomass that reduces the number of available binding sites [26]. Therefore, for further biosorption experiments, the optimum biomass dose was selected as 1.0 g/50 mL (20 g/L).

3.4. Effect of contact time and kinetic modeling

Contact time between biosorbent and adsorbate has a great influence on the biosorption process. Biosorption of Ni(II) with various initial concentrations (60, 100, and 120 mg/L) was carried out at various time intervals. The uptake capacities of CCM for Ni(II) at various concentrations monitored indicated that the maximum uptake capacities were achieved within 2 h for all three initial concentrations of Ni(II) (Fig. 5). Initially, the rate of biosorption was found to be rapid,

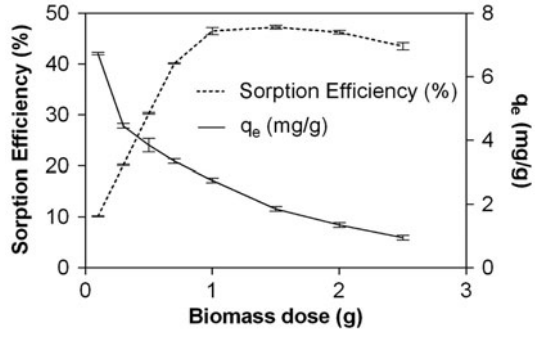

Fig. 4. The effect of biomass dose on the biosorption of Ni (II) by CCM as biosorbent (biomass dose = 0.1–2 g/50 mL; Ni(II) concentration = 120 mg/L).

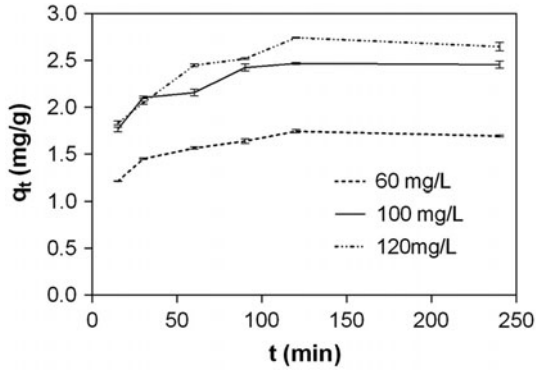

Fig. 5. The effect of contact time on the biosorption of Ni (II) using CCM as biosorbent (biomass dose = 1.0 g/50 mL; Ni(II) concentrations = 60, 100, and 120 mg/L).

then became slower and reached equilibriums at around only 2 h [27]. The required batch time of less than 2 h may facilitate the nickel removal process for potential applications of the CCM biosorbent in wastewater treatment. This experiment suggests that a contact time of around 2 h is optimal for the biosorption of Ni(II). Thus, for the next biosorption experiment, a contact time of 120 min (2 h) was applied.

To design a batch biosorption system, a model to predict the behavior of the biosorption rate is quite important. In order to study the kinetics of Ni(II) biosorption onto the CCM biosorbent, different kinetic models including pseudo-first-order, pseudo-second-order, and intraparticle diffusion models were employed. On the basis of correlation coefficient (R^2) values, the model that shows the best fit for experimental data was determined. The pseudo-first-order model can be expressed as:

$$\frac{dq}{dt} = k_1(q_e - q_t) \tag{3}$$

where q_e and q_t are the amounts of Ni(II) ions adsorbed (mg/g) by CCM at equilibrium and time t, respectively. k_1 is the rate constant of this model with the unit of min^{-1}. On integration by applying the conditions $q_t = 0$ at $t = 0$ and $q_t = q_t$ at $t = t$, Eq. (3) can be written as follows:

$$\log\,(q_e - q_t) = \log q_e - \frac{k_1}{2.303}(t) \tag{4}$$

This model is applicable only if the plot of log $(q_e - q_t)$ vs. t gives a straight line. From this straight line, the values of intercept and slope can be determined. The pseudo-second-order model can be expressed as:

$$\frac{dq}{dt} = k_2(q_e - q_t)^2 \tag{5}$$

where k_2 (g mg^{-1} min^{-1}) is the pseudo-second-order rate constant and t is contact time (min). On integration by applying the conditions $q_t = 0$ at $t = 0$ and $q_t = q_t$ at $t = t$, Eq. (5) can be written as follows:

$$\frac{t}{q_t} = \frac{1}{k_2 q_e^2} + \frac{t}{q_e} \tag{6}$$

If the second-order kinetic model is applicable, then a plot of t/q_t vs. t will give a straight line.

In order to investigate the kinetics of Ni(II) adsorption onto CCM, both pseudo-first- and second-order kinetic models were applied on the experimental data. By plotting the graphs for pseudo-first- and second-order, values of different parameters (such as values

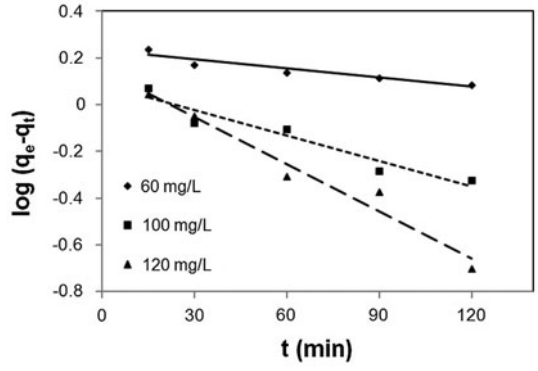

Fig. 6. The plot of pseudo-first-order model for the biosorption at various concentrations Ni(II) onto CCM (biomass dose = 1.0 g/50 mL; Ni(II) concentrations = 60, 100, and 120 mg/L).

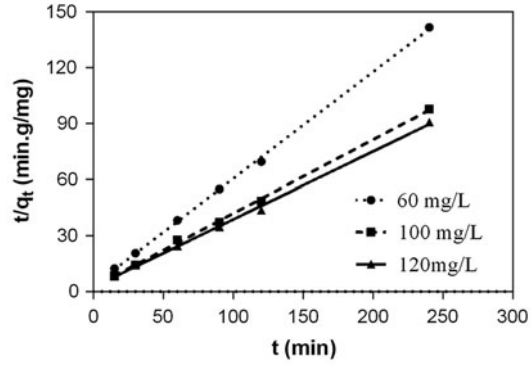

Fig. 7. The plot of pseudo-second-order model for the biosorption of Ni(II) onto CCM (experimental biomass dose = 1.0 g/50 mL; Ni(II) concentrations = 60, 100, and 120 mg/L).

of q_e, k_1, k_2, and R^2) were calculated. Results for the pseudo-first-order kinetic model are presented for three different concentrations (60, 100, and 120 mg/L) of Ni(II) in Fig. 6 and the values for different parameters are given in Table 2. The values of correlation coefficient were found to be unsatisfactory ($R^2 < 0.99$), and the values of $q_{e,\ cal}$ were found to be far less than the $q_{e,\ exp}$ values, indicating that the pseudo-first-order kinetic model may not be suitable to describe the kinetics of the Ni(II) biosorption.

The results for the pseudo-second-order kinetics are presented for three different concentrations (60, 100, and 120 mg/L) of Ni(II) in Fig. 7, and the values of different parameters are presented in Table 2. The values of correlation coefficient (R^2) and $q_{e,\ cal}$ were found to be in a better agreement with the experimentally determined values ($q_{e,\ exp}$) when compared to values from the pseudo-first-order model (Table 2). Therefore, it was concluded that the pseudo-second-order kinetics can be used to describe the biosorption of Ni(II) onto CCM. These results indicate that biosorption of Ni(II) onto CCM depends on the concentration of Ni(II) and furthermore, the rate determining step involves chemical biosorption [28]. The pseudo-second-order kinetics also suggests that the key interaction between the Ni(II) and the CCM involves their sharing of valence electrons.

The biosorption of Ni(II) onto CCM probably involves three major steps as follows. First, Ni(II) migrates from a bulk solution through a layer of liquid surrounding the external surface of CCM. Upon approaching the external surface of CCM, the ion is rapidly bound to the CCM. After that, Ni(II) diffuses to an adsorption site via a pore diffusion process which could be one of the rate limiting steps, along with the mass transfer of the ion across the layer of liquid in the first step [29]. The valence electrons on the oxygen atoms of the functional groups such as hydroxyl and carboxylate groups of CCM can be shared and form bonds with Ni(II) at the active sites of CCM. To investigate whether the intraparticle diffusion process is the rate limiting step, the intraparticle diffusion model is used to analyze the kinetic data. The intraparticle diffusion model is shown in the following equation:

$$q_t = k_{id} t^{1/2} + C \tag{7}$$

where k_{id} (mg g^{-1} min$^{-1/2}$) is the rate constant of the intraparticle diffusion model and C is the intercept that gives information about the thickness of the boundary layer [30]. According to this model, if the plot of $t^{1/2}$ vs. q_t produces a linear graph over the whole range of contact time and it passes through the origin, then intraparticle diffusion is the sole rate determining step in biosorption of Ni(II) onto CCM [29,31]. The plot for the intraparticle diffusion model is presented in Fig. 8 and the calculated parameters are presented in Table 3. The plot was not found to be linear over the entire range and the line did not pass through the origin, indicating that the intraparticle diffusion is not the only rate controlling step as boundary layer diffusion also participates to some extent in

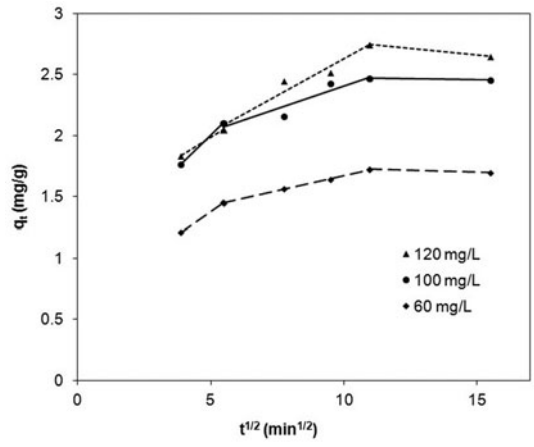

Fig. 8. The plot for the intraparticle diffusion model for the biosorption of Ni(II) onto CCM (biomass dose = 1.0 g/50 mL; Ni(II) concentrations = 60, 100, and 120 mg/L; contact time = 15–240 min).

Table 2
Parameters of pseudo-first- and second-order kinetic models

		Pseudo-first-order kinetics			Pseudo-second-order kinetics		
Conc. (mg/L)	$q_{e,\ exp}$ (mg/g)	k_1 (min^{-1})	$q_{e,\ cal}$ (mg/g)	R^2	k_2 (g mg^{-1} min^{-1})	$q_{e,\ cal}$ (mg/g)	R^2
60	1.724	5.645×10^{-4}	0.632	0.902	0.099	1.746	0.999
100	2.468	1.563×10^{-3}	1.072	0.925	0.061	2.536	1.000
120	2.706	2.909×10^{-3}	0.829	0.967	0.052	2.761	0.999

Table 3
Parameters for intraparticle diffusion model

	Intraparticle diffusion model		
Conc. (mg/L)	$k_{id,1}$ (mg g^{-1} min^{-1})	$k_{id,2}$ (mg g^{-1} min^{-1})	$k_{id,3}$ (mg g^{-1} min^{-1})
60	0.1496	0.0492	−0.0066
100	0.2126	0.0738	−0.0026
120	0.1340	0.1202	−0.0214

Ni(II) biosorption onto the CCM biosorbent [32]. The multilinearities in each plot evidently demonstrated that multiple processes collectively involved in controlling rate of the Ni(II) biosorption onto the CCM biosorbent throughout the time course. The first part corresponds to transfer of Ni(II) ions onto external surface of CCM by diffusion which is the fastest step with the highest $k_{id,1}$ values (Table 3). The second portion of the plots are slower with the lower $k_{id,2}$ (Table 3), and it corresponds to pore or intraparticle diffusion in which Ni(II) ions diffuses from external biomass surface into pores. The slowest step found in the third portion of the plots could corresponds to the equilibrium for which the pore diffusion was offset due to the low Ni(II) concentration [29]. In summary, both intraparticle diffusion and the equilibrium of adsorption can be the rate limiting step. At the initial period of adsorption, the intraparticle diffusion was the rate limiting step. As the time proceeded, the concentration of Ni(II) in solution was lowered and the adsorption process started to slow down since it was approaching the equilibrium of adsorption.

3.5. Effect of initial metal ion concentration and adsorption isotherm study

The results for the effect of initial Ni(II) ion concentration on the biosorption process presented in Fig. 9 shows that as the initial metal ion concentration increased, metal uptake capacity (mg/g) increased and then reached a saturation point at a concentration value of around 120 mg/L. This increase could be explained on the basis of the fact that as the concentration of Ni(II) increases, the chances of collision between metal ions and binding sites also increases, and hence the biosorption increases [33].

In order to investigate the interaction between metal ions and biomass, adsorption isotherm study is an important means. Although several isotherm models have been used, the Langmuir and Freundlich isotherm models, due to their simplicity, are most widely used. The Langmuir isotherm model assumes that the binding sites are equally distributed for biosorption, there is no interaction between adsorbed metal ions,

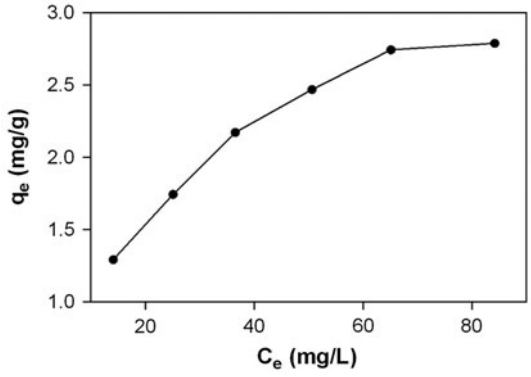

Fig. 9. The effect of initial metal ion concentration on the biosorption of Ni(II) using CCM as biosorbent (biomass dose = 1.0 g/50 mL; Ni(II) concentrations = 40–140 mg/L).

and after saturation of biomass, a monolayer is formed [34]. The equation describing the Langmuir isotherm model is shown in the following equation:

$$q_e = q_{max}\frac{K_L C_e}{1 + K_L C_e} \tag{8}$$

where q_e (mg/g) is the metal uptake capacity of biomass at equilibrium, q_{max} (mg/g) is the maximum monolayer biosorption capacity, C_e (mg/L) is the metal ion concentration at equilibrium, and K_L (L/mg) is the Langmuir constant. The linearized form can be written as follows:

$$\frac{C_e}{q_e} = \frac{C_e}{q_{max}} + \frac{1}{K_L q_{max}} \tag{9}$$

By plotting the graph of C_e/q_e vs. C_e, the isotherm constants can be calculated from the slope and intercept of this plot if it is a straight line. The Freundlich isotherm model assumes that the binding sites are not equally distributed and biosorption takes place in a heterogeneous fashion [30]. The equation describes the Freundlich isotherm model is shown in the following equation:

$$q_e = K_f C_e^{1/n} \quad (10)$$

where K_f is the constant related to biosorption capacity (mg/g) and $1/n$ represents the biosorption intensity. The Freundlich isotherm model in linearized form can be written as:

$$\log q_e = \log K_f + \frac{1}{n}\log C_e \quad (11)$$

The linearized and non-linearized plots for the Langmuir and Freundlich isotherm models are plotted in Figs. 10–12. The calculated parameter values from the linearized Langmuir and Freundlich isotherms are presented in Table 4. According to the table, the maximum uptake capacity (q_{max}) of CCM biomass for Ni (II) was found to be at 3.77 mg/g. The higher values of q_{max} and R^2 suggest that the Langmuir isotherm

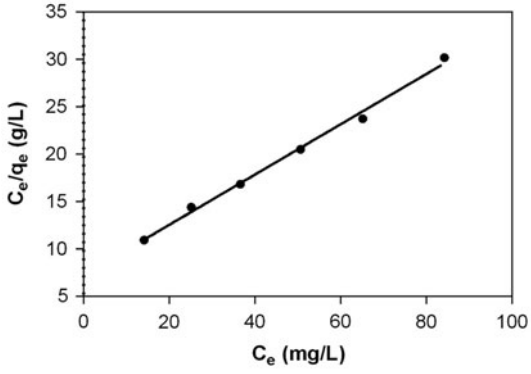

Fig. 10. The linearized Langmuir isotherm plot for the biosorption of Ni(II) onto the CCM biosorbent.

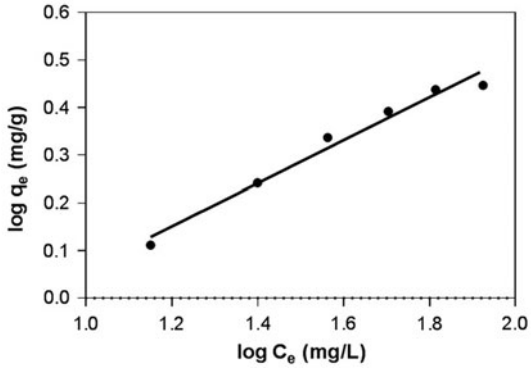

Fig. 11. The linearized Freundlich isotherm plot for the Ni (II) biosorption onto the CCM biosorbent.

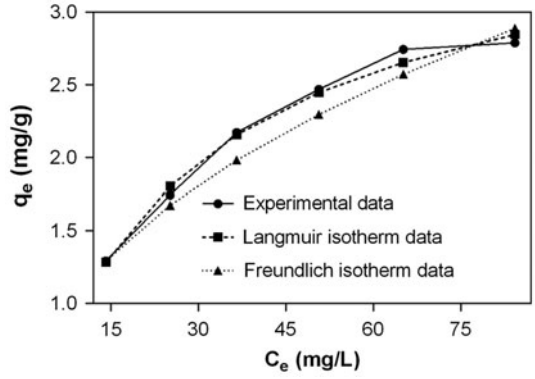

Fig. 12. The comparisons of non-linearized experimental, Langmuir and Freundlich isotherms for the Ni(II) biosorption onto the CCM biosorbent.

Table 4
Langmuir and Freundlich isotherm constants for biosorption of Ni(II) onto CCM

Langmuir constants			Freundlich constants		
$q_{max\ (cal)}$ (mg/g)	K_L	R^2	K_f (mg/g)	n	R^2
3.77	0.036	0.994	0.408	2.216	0.976

Table 5
Comparison of maximum uptake capacity for Ni(II) on different biosorbents

Biosorbent	q_{max} (mg/g)	Reference
Pleurotus ostreatus spent mushroom	3.04	[35]
Ficus religiosa (peepal) leaves	6.35	[36]
Peanut hulls	2.2	[37]
Brewer's yeast	5.34	[38]
CCM	3.77	Present study

model is more suitable to describe the biosorption of Ni(II) onto CCM when compared to the Freundlich isotherm model. The value of n (2.216) in the Freundlich isotherm model was found to be greater than one, indicating a favorable adsorption process. A comparison of q_{max} values of CCM with other biosorbents is given in Table 5.

3.6. Thermodynamic studies

The adsorption of Ni(II) was performed at different temperatures to observe the effect of temperature on

the adsorption. The thermodynamic parameters can be used to describe the process and also provide some information about the adsorption mechanism. The thermodynamic parameters including a change in free energy (ΔG°), a change in enthalpy of biosorption (ΔH°) and a change in entropy (ΔS°), were calculated by the following equations:

$$\Delta G^{\circ} = -RT \ln K \tag{12}$$

$$\Delta G^{\circ} = \Delta H^{\circ} - T\Delta S^{\circ} \tag{13}$$

where K is the equilibrium constant obtained from the Langmuir constant, K_L, with the dimension of L/mol [39,40]. The Langmuir parameters, K_L and q_{max}, for different adsorption temperatures were obtained by linear regression method as discussed in the previous section. The Langmuir parameters and ΔG° calculated by Eq. (12) are reported in Table 6.

Eqs. (12) and (13) can be combined to obtain the following equation:

$$\ln (K) = \frac{\Delta S^{\circ}}{R} - \frac{\Delta H^{\circ}}{RT} \tag{14}$$

Eq. (14) indicates a linear relationship between ln (K) and $1/T$. Fig. 13 shows the plot and linear regression of ln (K) vs. $1/T$. The slope of the linear equation is $-\Delta H^{\circ}/R$ and the y-intercept is $\Delta S^{\circ}/R$.

Table 6
Langmuir isotherm parameters and ΔG°

	Temperature (K)		
Parameter	288	308	318
K_L (L/mg)	0.0529	0.0877	0.1010
q_{max} (mg/g)	3.4048	2.3804	2.6567
K (L/mol)	3,106	5,146	5,929
ΔG° (kJ/mol)	−19.25	−21.88	−22.969

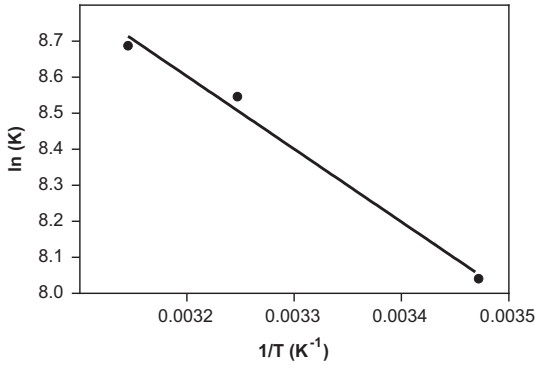

Fig. 13. Linear regression of ln(K) on $1/T$.

From the regression analysis, ΔH° and ΔS° were found to be 16.77 kJ/mol and 125.2 J/mol-K, respectively. The negative values of ΔG° indicate that the adsorption process is spontaneous. The positive value of ΔH° indicates that the adsorption of Ni(II) onto the CCM biomass is an endothermic process. The value of ΔH° is in the range of 2.1–20.9 kJ/mol which implies that the adsorption of Ni(II) onto CCM was mainly by a physical adsorption [41]. The small positive value of ΔS° indicates a slight increase in the randomness at the solid-solution interface during the adsorption process [42]. It should be noted that the values of thermodynamic parameters found in this study are in the ranges of the previously reported values [41,42].

3.7. Desorption studies

The desorption of Ni(II) from the biomass adsorbent was performed to examine the potential for the reuse and safe disposal of the biosorbent. 0.1 M HNO_3 (aq.) was used to desorb Ni(II) from the adsorbed biomass. HNO_3 is a good desorbing agent since it could desorb almost 100% of adsorbed Ni(II) from the biosorbent. The acid is a good desorbing agent because H^+ ions have affinity to attach to the functional groups on the biomass, and thus compete with the binding of the Ni(II) ions. Similarly, the desorption of Ni(II) from the biosorbent prepared from the husk of *Lathyrus sativus* by HNO_3 (aq.) was also reported by Panda et al. [43].

3.8. Effect of competing ions

Ni(II) biosorption was studied in the presence and absence of competing ions to elucidate their effect on the Ni(II) biosorption. Fig. 14 shows the effect of varying concentrations of competing ions on the Ni(II) biosorption. The concentrations of competing ions (Pb(II) and Co(II)) were in the range of 40–140 mg/L, while the concentration of Ni(II) was kept constant at 120 mg/L. The results in Fig. 14 shows that as the concentration of competing ions increased, the Ni(II) biosorption decreased. The presence of Pb(II) shows a more pronounced negative effect on the Ni(II) biosorption when compared to Co(II). This observation might be due to the higher atomic weight (207.21 g/mol) and ionic radii (132 pm) of Pb(II) as compared to the atomic weight (58.93 g/mol) and ionic radii (88.5 pm) of Co(II). Similar results were observed in the case of the

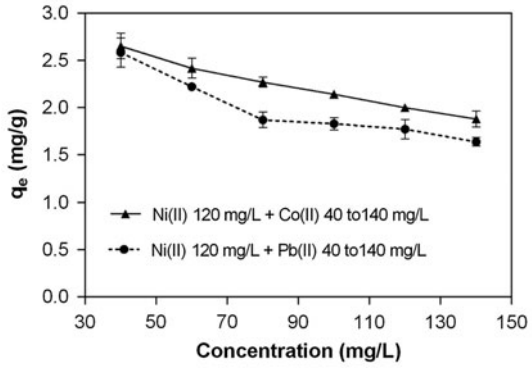

Fig. 14. The effect of varying concentrations of competing ions on the biosorption of Ni(II) onto the CCM biosorbent (120 mg/L of Ni(II) + 40–140 mg/L of Pb(II) or Co(II); biomass dose = 1.0 g/50 mL).

presence of Cd(II) as competing ion on Ni(II) biosorption using *Chlorella vulgaris*. The extent of decrease in biosorption becomes more pronounced with an increase in the concentration of competing ions [22].

4. Conclusion

The biosorption of Ni(II) on CCM was accomplished within 2 h at pH 5.0. The amount of Ni(II) biosorption increased with an increase in initial concentration of Ni(II) ions. A Langmuir isotherm model better described the adsorption process when compared with a Freundlich isotherm. The maximum monolayer adsorption capacity of the CCM biosorbent for Ni(II) was 3.77 mg/g. Adsorption of Ni(II) followed pseudo-second-order kinetics. Based on the thermodynamic studies, the adsorption of Ni(II) ions onto CCM biomass was an endothermic process which mainly involved a physical adsorption. In addition, the slight decrease in the equilibrium pH suggested that an ion-exchange also took place during the adsorption process. In addition, it was also possible to desorb almost all of the Ni(II) adsorbed on the biomass; therefore, CCM biomass possesses the potential for the reuse and safe disposal. Furthermore, biosorption of Ni(II) was found to decrease in the presence of competing ions. SEM shows submicrometer size structures on porous surface of the prepared CCM sorbent. On the basis of the above results and the ease of the CCM processing into a sorbent, it could be concluded that the biosorption of Ni(II) by CCM as a sorbent provides a potential inexpensive method to remove Ni(II) ions from wastewater.

Acknowledgment

This research was supported by the Thammasat University Research Fund and the National Research University Project of Thailand, Office of Higher Education Commission. We thank Mr Paul Vincent Neilson for editing this manuscript.

List of all symbols and abbreviations

$1/n$	—	biosorption intensity in the Freundlich isotherm model
AAS	—	atomic absorption spectroscopy
C	—	graph intercept in the intraparticle diffusion model
C_1	—	initial concentration
C_2	—	final concentration
CCM	—	coconut copra meal
C_e	—	metal ion concentration at equilibrium
Co(II)	—	cobalt (II) ions
EDX	—	energy-dispersive X-ray spectroscopy
k_1	—	rate constant of the pseudo-first-order model
k_2	—	rate constant of the pseudo-second-order model
K_f	—	constant related to biosorption capacity in the Freundlich isotherm model
k_{id}	—	rate constant of the intraparticle diffusion model
K_L	—	langmuir constant in the Langmuir isotherm model
Ni(II)	—	nickel (II) ions
Pb(II)	—	lead (II) ions
q_e	—	metal ion uptake capacity at equilibrium
q_{max}	—	maximum ion uptake capacity
q_t	—	metal uptake ion capacity at time t
R^2	—	correlation coefficient
SEM	—	scanning electron microscopy
t	—	contact time
V	—	solution volume
WHO	—	World Health Organization

References

[1] N. Akhtar, J. Iqbal, M. Iqbal, Removal and recovery of nickel (II) from aqueous solution by loofa sponge-immobilized biomass of *Chlorella sorokiniana*: Characterization studies, J. Hazard. Mater. 108 (2004) 85–94.

[2] A. Magyarosy, R.D. Laidlaw, R. Kilaas, C. Echer, D.S. Clark, J.D. Keasling, Nickel accumulation and nickel oxalate precipitation by *Aspergillus niger*, Appl. Microbiol. Biotechnol. 59 (2002) 382–388.

[3] J.S. Patel, P.C. Patel, K. Kalia, Isolation and characterization of nickel uptake by nickel resistant bacterial isolate (NiRBI), Biomed. Environ. Sci. 19 (2006) 297–301.

[4] S. Sarkar, A. Satheshkumar, R. Jayanthi, R. Premkumar, Biosorption of nickel by live biomass of *Trichoderma harzianum*, Res. J. Agr. Sci. 1 (2010) 69–74.

[5] M. Costa, K. Salnikow, S. Cosentino, C.B. Klein, X. Huang, Z. Zhuang, Molecular mechanisms of nickel carcinogenesis, Environ. Health Perspect. 102 (1994) 127–130.
[6] WHO, Guidelines for Drinking-water Quality, World Health Organization, Geneva, 2011.
[7] A. Saeed, M. Iqbal, Bioremoval of cadmium from aqueous solution by black gram husk (*Cicer arientinum*), Water Res. 37 (2003) 3472–3480.
[8] M. Ajmal, R.A.K. Rao, R. Ahmad, J. Ahmad, Adsorption studies on *Citrus reticulata* (fruit peel of orange): Removal and recovery of Ni(II) from electroplating wastewater, J. Hazard. Mater. 79 (2000) 117–131.
[9] F.A.A. Al-Rub, M.H. El-Naas, F. Benyahia, I. Ashour, Biosorption of nickel on blank alginate beads, free and immobilized algal cells, Process Biochem. 39 (2004) 1767–1773.
[10] J.P.K. Wong, Y.S. Wong, N.F.Y. Tam, Nickel biosorption by two chlorella species, *C. Vulgaris* (a commercial species) and *C. Miniata* (a local isolate), Bioresour. Technol. 73 (2000) 133–137.
[11] F. Veglio, F. Beolchini, Removal of metals by biosorption: A review, Hydrometallurgy 44 (1997) 301–316.
[12] M.N. Zafar, R. Nadeem, M.A. Hanif, Biosorption of nickel from protonated rice bran, J. Hazard. Mater. 143 (2007) 478–485.
[13] N. Ahalya, T.V. Ramachandra, R.D. Kanamadi, Biosorption of heavy metals, Res. J. Chem. Environ. 7 (2003) 71–79.
[14] T.J. Beveridge, R.G.E. Murray, Sites of metal deposition in the cell wall of *Bacillus subtilis*, J. Biotechnol. 141 (1980) 876–887.
[15] Y.-S. Ho, A.E. Ofomaja, Biosorption thermodynamics of cadmium on coconut copra meal as biosorbent, Biochem. Eng. J. 30 (2006) 117–123.
[16] S. Saittagaroon, S. Kawakishi, M. Namiki, Characterisation of polysaccharides of copra meal, J. Sci. Food Agric. 34 (1983) 855–860.
[17] A.E. Ofomaja, Y.S. Ho, Effect of pH on cadmium biosorption by coconut copra meal, J. Hazard. Mater. 139 (2007) 356–362.
[18] R. Aravindhan, B. Madhan, J.R. Rao, B.U. Nair, T. Ramasami, Bioaccumulation of chromium from tannery wastewater: An approach for chrome recovery and reuse, Environ. Sci. Technol. 38 (2004) 300–306.
[19] D. Park, Y.-S. Yun, J.M. Park, Studies on hexavalent chromium biosorption by chemically-treated biomass of *Ecklonia* sp., Chemosphere 60 (2005) 1356–1364.
[20] P. Ahuja, R. Gupta, R.K. Saxena, Zn^{2+} biosorption by *Oscillatoria anguistissima*, Process Biochem. 34 (1999) 77–85.
[21] A. Sarı, M. Tuzen, Biosorption of Pb(II) and Cd(II) from aqueous solution using green alga (*Ulva lactuca*) biomass, J. Hazard. Mater. 152 (2008) 302–308.
[22] Z. Aksu, G. Dönmez, Binary biosorption of cadmium (II) and nickel(II) onto dried *Chlorella vulgaris*: Co-ion effect on mono-component isotherm parameters, Process Biochem. 41 (2006) 860–868.
[23] A.V. AjayKumar, N.A. Darwish, N. Hilal, Study of various parameters in the biosorption of heavy metals on activated sludge, World Appl. Sci. J. 5 (2009) 32–40.
[24] P. Aikpokpodion, R. Ipinmoroti, S. Omotoso, Biosorption of nickel (II) from aqueous solution using waste tea (*Camella cinencis*) materials. Am.-Eurasian J. Toxicol. Sci. 2 (2010) 72–82.
[25] K. Kadirvelu, C. Faur-Brasquet, P.L. Cloirec, Removal of Cu(II), Pb(II), and Ni(II) by adsorption onto activated carbon cloths, Langmuir 16 (2000) 8404–8409.
[26] S. Karthikeyan, R. Balasubramanian, Evaluation of the marine algae *Ulva fasciata* and *Sargassum* sp. for the biosorption of Cu(II) from aqueous solutions, Bioresour. Technol. 98 (2007) 452–455.
[27] R.A.K. Rao, M.A. Khan, F. Rehman, Utilization of Fennel biomass (*Foeniculum vulgari*) a medicinal herb for the biosorption of Cd(II) from aqueous phase, Chem. Eng. J. 156 (2010) 106–113.
[28] Y.S. Ho, G. McKay, Pseudo second order model for sorption processes, Process Biochem. 34 (1999) 451–465.
[29] W.H. Cheung, Y.S. Szeto, G. McKay, Intraparticle diffusion processes during acid dye adsorption onto chitosan, Bioresour. Technol. 98 (2007) 2897–2904.
[30] D. Ozdes, A. Gundogdu, B. Kemer, C. Duran, M. Kucuk, M. Soylak, Assessment of kinetics, thermodynamics, and equilibrium parameters of Cr(VI) biosorption onto *Pinus brutia* TEN, Can. J. Chem. Eng. 9999 (2013) 1–9.
[31] M.E.H. Ahamed, X.Y. Mbianda, A.F. Mulaba-Bafubiandi, L. Marjanovic, Ion imprinted polymers for the selective extraction of silver(I) ions in aqueous media: Kinetic modeling and isotherm studies, React. Funct. Polym. 73 (2013) 474–483.
[32] B.H. Hameed, M.I. El-Khaiary, Malachite green adsorption by rattan sawdust: Isotherm, kinetic and mechanism modeling, J. Hazard. Mater. 159 (2008) 574–579.
[33] G. Çetinkaya Dönmez, Z. Aksu, A. Öztürk, T. Kutsal, A comparative study on heavy metal biosorption characteristics of some algae, Process Biochem. 34 (1999) 885–892.
[34] M.V. Subbaiah, Y.S. Yun, Biosorption of nickel(II) from aqueous solution by the fungal mat of *Trametes versicolor* (rainbow) biomass: Equilibrium, kinetics, and thermodynamic studies, Biotechnol. Bioprocess Eng. 18 (2013) 280–288.
[35] C.C. Tay, H.H. Liew, G. Redzwan, S. K. Yong, S. Surif, S. Abdul-Talib, *Pleurotus ostreatus* spent mushroom compost as green biosorbent for nickel (II) biosorption, Water Sci. Technol. 64 (2011) 2425–2432.
[36] Z.A. Muhammad, N. Ramzan, S. Naveed, N. Feroze, Ni(II) removal by biosorption using *Ficus religiosa* (peepal) leaves, J. Chil. Chem. Soc. 55 (2010) 81–84.
[37] F.D. Oliveira, A.C. Soares, O.M. Freitas, S.A. Figueiredo, Copper, nickel and zinc removal by peanut hulls: Batch and column studies in mono, tri-component systems and with real effluent, Global NEST J. 12 (2010) 206–214.
[38] L. Cui, G. Wu and T.S.Jeong, Adsorption performance of nickel and cadmium ions onto brewer's yeast, Can. J. Chem. Eng. 88 (2010) 109–115.
[39] C.C.V. Cruz, A.C.A. da Costa, C.A. Henriques, A.S. Luna, Kinetic modeling and equilibrium studies during cadmium biosorption by dead *Sargassum* sp. biomass, Bioresour. Technol. 91 (2004) 249–257.
[40] Y. Liu, Is the free energy change of adsorption correctly calculated?, J. Chem. Eng. Data 54 (2009) 1981–1985.
[41] Y. Liu, Y.-J. Liu, Biosorption isotherms, kinetics and thermodynamics, Sep. Purif. Technol. 61 (2008) 229–242.

[42] Z. Aksu, Determination of the equilibrium, kinetic and thermodynamic parameters of the batch biosorption of nickel (II) ions onto *Chlorella vulgaris*, Process Biochem. 38 (2002) 89–99.

[43] G.C. Panda, S.K. Das, T.S. Bandopadhyay, A.K. Guha, Adsorption of nickel on husk of *Lathyrus sativus*: Behavior and binding mechanism, Colloids Surf., B 57 (2007) 135–142.